Research Square

Preprints are preliminary reports that have not undergone peer review.
They should not be considered conclusive, used to inform clinical practice,
or referenced by the media as validated information.

Limited T-cell presence despite extensive microglial HLA class II expression in the frontal cortex in Alzheimer's disease

Sebastiaan Moonen
VIB
Simona Ospitalieri
KU Leuven
Rik Vandenberghe
KU Leuven
Dietmar Rudolf Thal
KU Leuven
Bart Strooper
bart.destrooper@kuleuven.be

VIB

Research Article

Keywords: Adaptive immunity, innate immunity, Alzheimer's disease, T cells, microglia, antigen presentation

Posted Date: November 5th, 2026

DOI: https://doi.org/10.21203/rs.3.rs-11446407/v1

License: This work is licensed under a Creative Commons Attribution 4.0 International License.
Read Full License

Additional Declarations: Competing interest reported. SM has no competing interests. SO has no competing interests. RVs institution has clinical trial agreements (RV as site PI) with Alector, AviadoBio, Biogen, Bristol-Myers Squibb, Denali, EliLilly, Johnson & Johnson, Merck, Roche and UCB. RV's institution has consultancy agreements with ACImmune and Novartis (RV as Data Safety Monitoring Board or Data Monitoring Committee member), and with Roche, EliLilly and AviadoBio (RV as member of international advisory board). DRT collaborated with Novartis Pharma AG (Switzerland), Fujirebio (Belgium), and GE-Healthcare (UK) and received consultant honoraria from Muna Therapeutics (Belgium). BDS is

consultant to Muna Therapeutics and is or has been consultant for Eli Lilly, Biogen, Janssen Pharmaceutica, Eisai, AbbVie and other biotech companies. B.D.S is a scientific founder of Augustine Therapeutics and a scientific founder and a minor stockholder of Muna Therapeutics.

Abstract

Background:

Upregulation of HLA class II in amyloid plaque-associated microglia is one of the most prominent immune-associated features of the Alzheimer's disease (AD) brain in large-scale human brain single nuclei RNA-sequencing and spatial transcriptomic data sets. This HLA class II response is part of a broader programme that includes co-stimulatory and co-inhibitory molecules involved in T-cell regulation. T-cell signatures are however sparse in these datasets.

Methods:

We therefore investigated whether the extensive upregulation of microglial HLA class II is accompanied by substantial T cell accumulation in a brain region with established AD pathology using immunohistology on postmortem brain tissue. We quantified CD3-, CD4- and CD8-positive T cells together with HLA-DR/DP/DQ-positive cells in the frontal cortex of symptomatic AD cases with confirmed local Aβ- and pTau-pathology, and in non-demented controls. Group differences in cell densities were assessed using binary logistic regression controlled for age and sex; regression analyses incorporating post-mortem interval were considered exploratory.

Results:

A striking numerical discrepancy between abundant HLA-DR/DP/DQ-positive microglia (on average 18 000 cells/cm^2) and very few parenchymal T cells (on average 8 cells/cm^2) in the AD frontal cortex is observed. We did not detect a significant increase in parenchymal T-cell numbers in AD compared with control cases which contrasted sharply with the dense T cell infiltrates observed in the positive-control ADEM case of acute disseminated encephalomyelitis.

Conclusions:

The central implication of our findings is that HLA class II expression in AD microglia should not automatically be equated with extensive T cell engagement in the brain parenchyma. It will require further molecular and spatial characterization to determine whether the rare parenchymal T cells that are present in AD, target specific antigens and have functional effects on the progression of AD. Further work is needed to discriminate the specific role of T-cells in AD versus other neurodegenerative disorders.

Background

Microglial expression of HLA class II is one of the most prominent immune-associated features of the Alzheimer's disease (AD) brain. HLA-DR-positive microglia surrounding amyloid-β (Aβ) plaques were already described in early neuropathological studies (1). More recent transcriptomic studies have confirmed that HLA class II genes are strongly induced in plaque-associated microglial states in AD (2–4). In affected grey matter, this HLA class II response is particularly concentrated around Aβ plaques, whereas HLA class II-positive microglia are more diffusely distributed in white matter (1, 5).

HLA class II molecules present peptide antigens to CD4 T cells with the help of HLA-associated co-stimulatory and co-inhibitory molecules (6). Recent work indicates that the plaque-associated HLA class II microglia also express those associated proteins (2–4). They furthermore present a diverse repertoire of peptides, rather than selectively presenting Aβ- or Tau-derived peptides, and they can interact with naive T-cells in an *in vitro* assay (3). These observations are compatible with the hypothesis that microglia interact with CD4 T cells. However, large-scale human brain single nuclei RNA-sequencing studies consistently demonstrate that T cells are a rare population in AD brain (7–10). Moreover, spatial transcriptomics did not detect lymphocyte infiltration in the brain parenchyma of AD patients (4). Experimental studies have further shown that key features of AD neuropathology can develop in systems lacking mature B and T lymphocytes (11–15).

To complement our transcriptomic investigations, we investigated here whether the extensive HLA class II response of microglia in AD is accompanied by substantial T cell accumulation using an immunohistological approach. We quantified CD3-, CD4- and CD8-positive T cells together with HLA-DR/DP/DQ-positive cells in the frontal cortex of 9 symptomatic AD cases with local Aβ plaque and Tau pathology, and in 10 non-demented controls.

Materials and Methods

Human autopsy cases

Postmortem brain samples from 20 patients were included in this study (**Supplementary Table 1**). Cases were selected from the UZ/KU Leuven Biobank after systematic application of the absence of encephalitis, meningitis or other major inflammatory disease affecting the CNS as predefined exclusion criterion. A case diagnosed with acute disseminated encephalomyelitis (ADEM) was included as positive control for T cell infiltration. Relevant clinical and pathological information was extracted from the clinical files of the patients included in this study and are summarized in **Supplementary Table 1**. The cerebrum, cerebellum, and brainstem were cut in equal parts along the right and left hemispheres. The right hemisphere of the cerebrum, cerebellum and right half of the brainstem were further dissected for gross neuropathological assessment and stored at -80°C. The left hemisphere of the cerebrum, cerebellum and left half of the brainstem were first fixed in 4% aqueous or phosphate-buffered formaldehyde during two to four weeks, followed by dissection and gross neuropathological assessment. Formalin-fixed brain samples were then collected from frontal, parietal and occipital lobe (Area 17), cingulate gyrus, hippocampus with temporal cortex, entorhinal cortex, hypothalamus, basal

ganglia, amygdala, basal nucleus of Meynert, thalamus, midbrain, pons, medulla oblongata and cerebellum.

Neuropathological assessment

Left hemisphere brain samples were embedded in paraffin and cut in 5 µm tissue sections using an electronic rotary microtome (Thermo Fisher Scientific). Tissue sections were mounted on Flex IHC adhesive microscope slides (Dako, Glostrup, Denmark) and dried at 55°C before storing in a microscope slide box at room temperature. For diagnostic purposes, sections were stained with hematoxylin and eosin (H&E). Neuropathological assessment of AD pathology was performed based on immunohistochemistry and scored according to the Aβ phases and Braak-neurofibrillary tangle (Braak-NFT) stages for the spread of Aβ and pTau throughout the brain, respectively (16–18). The Consortium to Establish a Registry for AD (CERAD) score was determined based on the neuritic plaque frequency (19). The National Institute of Aging-Alzheimer's Association (NIA-AA) score was determined based on the Aβ phase, Braak-NFT stage and CERAD score (20). Primary age-related tauopathy (PART) (21) was observed in two non-AD cases and the ADEM case. CDR scoring (22) was retrospectively performed based on the available clinical information of the patients as previously described (23) and used as measure for cognitive and functional impairment. Cases were assigned to the AD group based on the documented presence of dementia (CDR ≥ 0.5) and the presence of intermediate to high degrees of AD neuropathological changes (NIA-AA score). Cases without dementia symptoms (CDR = 0) and without co-occurring Aβ and pTau pathology (NIA-AA score = 0) were assigned to the non-AD control group.

Immunohistochemistry

Tissue sections from the frontal cortex were used for immunohistochemistry on AD and non-AD cases, while hippocampus with temporal cortex was used for the ADEM case, containing multiple local T cell infiltrations. CD3, CD4 and CD8 stainings were performed to investigate the presence of T cells. HLA-DR/DP/DQ was stained to investigate the HLA class II response. Aβ and pTau stainings were performed to confirm and quantify local AD neuropathology. Information on primary antibodies including dilutions can be found in **Supplementary Table 2**. Paraffin-embedded tissue sections were deparaffinized using an autostainer (Leica Biosystems), followed by heat-induced epitope retrieval using a PT Link module (pH 6.1, Dako). Hydrogen peroxide was used to quench endogenous peroxidase. Primary antibodies for HLA-DR/DP/DQ were incubated overnight at room temperature in a humid chamber, followed by horseradish peroxidase (HRP)-labeled secondary antibodies, and visualization using 3,3´-diaminobenzidine tetrahydrochloride hydrate (DAB). DAB-stained slides for HLA-DR/DP/DQ were then consecutively stained for CD4, CD3, Aβ or pTau using FastRed. Immunostaining for Aβ was preceded by treatment with formic acid for 3 minutes. Single stains for CD8 were performed using DAB, single stains for CD3 and CD4 were performed using FastRed. After immunostaining, slides were counterstained using hematoxylin, dehydrated using an autostainer (Leica Biosystems), and mounted with cover glasses using an automated cover-slipper (Leica Biosystems) and Leica CV mount (Leica Biosystems). Representative

images were captured using a Leica DFC7000 T camera (Leica Microsystems, Wetzlar, Germany) on a Leica DM2000 LED light microscope (Leica Microsystems). Images were processed using ImageJ software (National Institutes of Health, Bethesda, USA). Figures were made using Inkscape (https://inkscape.org/).

Quantification of local AD pathology and immunoreactive cells

For the quantification of local AD pathology and immunoreactive cells, DAB- and/or FastRed-stained tissue sections were imaged using a brightfield Marzhauser SlideExpress 2 slide scanner system (Nikon). Quantifications of Aβ deposition, accumulation of pTau, HLA-DR/DP/DQ-, CD3-, CD4-, and CD8-positive cells were then performed on whole-slide scans using QuPath. Briefly, frontal cortex grey matter was delineated, followed by thresholding or positive cell detection using the appropriate chromogen staining vectors. Positive cell detections were manually categorized as parenchymal cells depending on the spatial location in the tissue, based on the hematoxylin counterstain, checked for staining artefacts, and summarized per cm^2. Aβ deposition and pTau accumulation was summarized as the percentage of area with positive immunostaining.

Statistical analysis

Quantifications of Aβ, pTau, and immunoreactive cells are summarized as the percentage of area with positive immunostaining and the cells per cm^2 detected per case, respectively, together with the mean and SEM per group. Statistical testing was performed using R statistical software and GraphPad Prism 10 (GraphPad, San Diego, USA). Binary logistic regression with Firth's bias-reduced penalized-likelihood method for small sample sizes was performed in R, controlling for age and sex (complete sample size) (**Suppl. Table 3**) and age, sex and PMI (reduced sample size due to missing PMI data points) (**Suppl. Table 4**). For quantifications of the ADEM case, data were checked for normality, followed by the unpaired t-test (Welch's). Spearman correlation was computed using R, with and without Benjamini-Hochberg procedure to control for false discovery rate (FDR). Correlation was deemed moderate, and thus relevant, with r-values between 0.3 and 0.7 (24). Correlation higher than 0.7 was considered as high. Scatter plots were computed using GraphPad prism, showing how the number of parenchymal CD8 T cells and the number of HLA class II-positive cells relate to the Aβ-positive area and pTau-positive area (**Supplementary Fig. 4**). Multiple linear regression was performed using R. Statistical significance was defined as a p-value below 0.05.

Results

We performed immunostainings for T cell markers, HLA-DR/DP/DQ, amyloid-β (Aβ) and hyperphosphorylated Tau (pTau) pathology in the frontal cortex of 9 symptomatic Alzheimer's disease (AD) cases and 10 non-demented control cases (non-AD) (cohort information provided in **Supplementary Table 1**). Quantifications were performed on whole slide images as percentage of

positive area or as the number of positive cells per cm^2 of frontal cortical grey matter. Analysis was done using QuPath. Symptomatic AD cases had documented dementia and an intermediate to high degree of AD neuropathological changes. Non-AD cases were cognitively healthy and showed minimal Aβ or pTau pathology. Chromogen immunostainings showed a clear increase in Aβ (3.96 ± 0.62% area positive for 4G8) (Fig. 1a-c) and pTau pathology (0.48 ± 0.13% area positive for AT8) (Fig. 1d-h) in the frontal cortex of AD patients. HLA-DR/DP/DQ-positive cells were distributed throughout the frontal cortical parenchyma and clustering was observed of HLA-DR/DP/DQ-positive cells with microglial morphology at Aβ plaques (Fig. 1b-c), areas without pTau (Fig. 1e) and areas with neuritic pTau (Fig. 1f). Clustering of HLA class II-positive cells was not observed near pTau tangle-filled neuronal cell bodies (Fig. 1g, h) (1, 25–27). AD cases showed substantially more HLA-class II-positive cells (18.000 ± 3438 cells per cm^2) than non-AD cases (2538 ± 542 cells per cm^2, p = 0.005) (Fig. 1i). A case with acute disseminated encephalomyelitis (ADEM) was included as a positive control for brain T cell infiltration (**Supplementary Fig. 1**).

Increased numbers of HLA class II-positive cells are not accompanied by increased CD3-positive T cell numbers in AD frontal cortex

We next assessed the abundance of CD3-positive T cells using dual-chromogen immunostaining with FastRed for CD3 and with DAB for HLA-DR/DP/DQ. Parenchymal CD3-positive T cells were detected in 8 of 9 AD cases and 8 of 10 non-AD cases, whereas intravascular CD3-positive T cells were detected in all 9 AD cases and 9 out of 10 non-AD cases. The number of parenchymal CD3-positive T cells was not different between AD and non-AD cases (8.1 ± 3.0 versus 10.0 ± 4.7 cells per cm^2, respectively; p = 0.226) (Fig. 2a). Thus, despite an average density of approximately 18,000 HLA class II-positive cells/cm^2 in AD cortex, only approximately eight parenchymal CD3-positive T cells/cm^2 were detected. The ratio of HLA class II-positive cells to parenchymal CD3 T cells ranged from 1164 to 5205 HLA class II-positive cells per CD3 T cell in AD cases, while 53 to 660 HLA class II-positive cells per CD3 T cell were observed in non-AD cases, which showed a lower number of HLA class II-positive cells (Fig. 2b and Fig. 1i). Parenchymal CD3-positive T cells were only sporadically observed in both AD and non-AD cases (Fig. 2d, e), whereas CD3-positive T cells were readily observed in association with blood cells (Fig. 2d, f). Single staining for CD3 confirmed the very low density of CD3-positive T cells throughout the frontal cortical grey matter (Fig. 2g, h**)**.

CD4-positive T cells are rare in the frontal cortex of both AD and non-AD cases

Because HLA class II molecules canonically present antigens to CD4-positive T cells, we next assessed CD4-positive T cell abundance. Frontal cortical sections from AD and non-AD cases were co-stained for CD4 using FastRed and HLA-DR/DP/DQ using DAB. Parenchymal CD4-positive T cells were quantified per cm^2 on whole-slide images using QuPath.

Parenchymal CD4-positive T cell numbers were low in both groups and did not differ significantly between AD and non-AD cases (1.0 ± 0.5 versus 4.7 ± 2.2 cells per cm^2, respectively, p = 0.114 (Fig. 3a)). Parenchymal CD4-positive T cells were only rarely detected, being present in 5 of 9 AD cases and 4 of 10 non-AD cases (Fig. 3b and **c**). Intravascular CD4-positive T cells were detected in 3 of 9 AD cases and 6 of 10 non-AD cases. Single CD4 staining confirmed the scarcity of CD4-positive T cells in frontal cortical grey matter, while CD4-positive cells were readily detected in association with white-matter blood vessels, providing an internal positive control for the staining (Fig. 3d-g).

CD8-positive T cells constitute the predominant detectable parenchymal T cell population but remain sparse.

We next investigated whether CD8-positive T cells accounted for a substantial proportion of the parenchymal T cell populations. CD8 immunoreactivity was visualized using DAB and cells were quantified per cm^2 of frontal cortical grey matter using QuPath. Parenchymal CD8-positive T cell numbers were not significantly increased in AD cases compared to non-AD cases (4.5 ± 1.4 versus 1.4 ± 0.6 cells per cm^2, p = 0.266, Fig. 4a). These numbers are consistent with CD8-positive cells constituting a substantial proportion of the detectable parenchymal T cell population. Their absolute abundance nevertheless remained very low compared with that of HLA class II-positive cells.

Similar to CD3-positive T cells, parenchymal CD8-positive T cells were observed only sporadically throughout the frontal cortex and were detected in 8 of 9 AD cases and 6 of 10 non-AD cases (Fig. 4b and **c**). Intravascular CD8-positive T cells were associated with blood vessels in all 9 AD cases and 9 of 10 non-AD cases (Fig. 4d and **e**).

We then checked potential correlations between the number of parenchymal CD3, CD4 and CD8 T cells, the number of HLA class II-positive microglia, and Aβ (4G8)-positive and pTau (AT8)-positive area (**Supplementary Fig. 2**). Spearman correlation was performed with the Benjamini-Hochberg procedure to control the false discovery rate. Parenchymal CD8 T cells showed a moderate trend towards correlation (rho = 0.50, FDR p = 0.083) with pTau-positive area (**Supplementary Fig. 2**), significant when using unadjusted p-values (p = 0.028) (**Supplementary Fig. 3**). No correlation was found between parenchymal CD8 T cells and Aβ-positive area (**Supplementary Figs. 2 and 3**). HLA class II-positive microglia were strongly correlated with Aβ-positive area (rho = 0.71, FDR p = 0.004), and moderate correlation was observed between HLA class II-positive microglia and pTau-positive area (rho = 0.65, FDR p = 0.009) (Fig. 5). Multiple linear regression controlled for age, sex and PMI confirmed correlation between HLA class II-positive microglia and Aβ-positive area, HLA class II-positive microglia and pTau-positive area, CD8 T cells and pTau-positive area, and additionally showed correlation between CD8 T cells and HLA class II-positive microglia (**Suppl. Table 5**).

An ADEM case illustrates the contrast with overt T cell infiltration

To determine whether the low T cell density observed in AD reflected limited sensitivity of the staining approach, we examined a case of acute disseminated encephalomyelitis (ADEM) as a positive control for overt neuroinflammatory T cell infiltration. Using the same markers, dense CD3-, CD4-, and CD8-positive T cell infiltrates were readily detected together with abundant HLA-DR/DP/DQ-positive cells (**Supplementary Fig. 1a-c**). Across five selected areas of T cell infiltration, CD3-positive T cell densities reached several thousand cells/cm², compared with fewer than ten parenchymal CD3-positive T cells/cm² in the AD frontal cortex (**Supplementary Fig. 1d,e**). Thus, the sparse T cell presence observed in AD is readily distinguishable from the overt T cell accumulation detectable in acute neuroinflammatory disease using the same histopathological approach.

Discussion

The main finding of this study is the striking discrepancy between the abundance of HLA-DR/DP/DQ-positive microglia compared to the few parenchymal T cells in the AD frontal cortex. On average 18 000 HLA class II-positive cells per cm² were observed, compared with only 8 CD3-positive parenchymal T cells. Moreover, parenchymal T cell numbers were not increased in AD compared with control cases. In contrast, dense T cell infiltrates were observed in an acute disseminated encephalomyelitis case, indicating that T cells were readily detected by our method. The scarcity of CD4-positive T cells is intriguing, given the canonical role of HLA class II in antigen presentation to CD4 T cells, and the presence of antigen and HLA-associated co-stimulatory and co-inhibitory molecules on the microglia (6). Together, these findings indicate that extensive microglial HLA class II expression should not by itself be interpreted as evidence of widespread local T-cell engagement. The very low number of parenchymal T cells places an important quantitative constraint on how frequently such interactions could occur.

Our findings are consistent with previous observations showing limited presence of parenchymal T cells in the AD frontal cortex grey matter, white matter and entorhinal cortex (28, 29). Increased T cell numbers have, however, been reported in the AD hippocampus in association with pTau pathology (28, 30). Thus T cell presence may vary between brain regions and their anatomical, cellular and molecular specifics. An important limitation of our study is that T-cell density may be underestimated in formalin-fixed paraffin-embedded 5 µm sections, as antigen detection can be less sensitive than in thicker free-floating sections used in some previous studies (31, 32). Methodological differences in tissue processing, section thickness and staining sensitivity may therefore contribute to differences in absolute T-cell counts between studies and potential differences between disease and non-disease tissue, although they are unlikely to account for the several-orders-of-magnitude discrepancy between the abundance of HLA class II-positive microglia and parenchymal T cells observed here.

Vascular and meningeal compartments are important to consider, as CD8-positive T cells in perivascular spaces are associated with Aβ-positive blood vessels and leptomeninges (33, 34). This in turn, has implications for the interpretation of single nuclei RNA sequencing studies (7), where pending on the position of the brain sample taken, T cells from parenchyma and vasculature can get mixed up. Associations between T cells and pTau pathology have been reported in other neurodegenerative

conditions, in particular increased CD8 T cells are seen in FTLD-Tau, Pick's disease or progressive supranuclear palsy compared to controls (32, 35). Notably, the numbers of T cells are still substantially lower than for microglia (35). Thus, observations from selected regions or disease contexts should be interpreted carefully as available human neuropathological data do not establish widespread parenchymal T-cell infiltration across the AD brain.

The contrast with overt neuroinflammatory disease such as ADEM strengthen this point of view. Similarly, in active multiple sclerosis lesions, approximately one T cell is found for every 1.5 HLA class II-positive cell (21), whereas in the AD frontal cortex examined here, HLA class II-positive cells outnumbered parenchymal T cells by several orders of magnitude. Microglial nodules in multiple sclerosis are frequently accompanied by local T cell accumulation (21), whereas we did not observe comparable T-cell accumulations around the prominent HLA class II-positive clusters in the AD sections examined here.

It should be pointed out that the current observations do not exclude biologically meaningful interactions between the few parenchymal T cells and microglia or effects of such interactions on neurons (31, 33). However, such interactions can involve only a small fraction of the HLA class II-positive microglial population at any given time and interpretation of data need to take into account this quantitative discrepancy. It is possible that the low numbers of T cells in the brain parenchyma simply reflect activated T cells patrolling the nervous system (36). This is particularly relevant in light of recent evidence that plaque-associated human microglia express a broad antigen-presentation programme and present a diverse peptide repertoire that is not dominated by Aβ- or tau-derived peptides (3). T cell responses to neural autoantigens appear largely preserved in AD compared with age-matched controls (37). The extensive HLA class II response of Aβ-plaque associated microglia may therefore reflect a broader state of immune surveillance and regulation and should not necessarily be interpreted as evidence of widespread conventional antigen presentation to infiltrating T cells (3). The upregulation of MHC class II molecules by microglia around Aβ plaques could also be the consequence of exposure to IFN-γ secreted by T cells located in dura or vascular borders, rather than adaptive immune cells infiltrating deep in the parenchyma.

Clonally expanded CD8 T cells have been reported in the cerebrospinal fluid of patients with AD (27), and CD8-positive cells constitute the predominant T-cell subset detected in our frontal cortex samples. Recent work in a mouse model of tauopathy showed that peripheral cDC1-dependent antigen cross-presentation is required for efficient priming and brain accumulation of CD8 T cells and contributes to tau-mediated neurodegeneration (33). These findings provide an important mechanism by which CD8 T cells may contribute to neurodegeneration without necessarily implying that plaque-associated HLA class II-positive microglia are their primary activating antigen-presenting cells. In our human frontal cortex samples, however, parenchymal CD8 T-cell numbers remained low. Their accumulation may vary between brain regions and could be influenced by vascular pathology: APOE4 is associated with pericyte degeneration and blood-brain barrier dysfunction (34), and increased brain CD8 T-cell accumulation has been reported in mice expressing human APOE4 (30). Thus, the contribution of CD8 T cells may depend

on disease context, brain region and vascular co-pathology, while remaining compatible with the limited parenchymal T-cell presence observed here.

Further studies in independent and larger cohorts will be necessary to further investigate the reported increases of T cells in other brain areas, and how their presence is modulated by co-morbidities, in particular vessel pathology. Post-mortem interval may also influence tissue preservation and detection of lymphocytes, and was therefore explored as a covariate. PMI showed no consistent association with parenchymal T-cell measures, although an association with CD8-positive T-cell density was observed in one regression model. Given the small cohort and wide confidence intervals, these analyses should be considered exploratory.

Conclusions

The central implication of our findings is that HLA class II expression in human AD microglia should not automatically be equated with extensive T cell engagement in the brain parenchyma. Determining whether the rare T cells have specific antigenic targets or functional effects in AD will require direct molecular and spatial characterization. Further work should determine how T-cell involvement varies across brain regions, disease stages and different neurodegenerative disorders.

Abbreviations

Abbreviation	Definition
Aβ	Amyloid-beta
ADEM	Acute disseminated encephalomyelitis
AD	Alzheimer's disease
AGD	Argyrophilic grain disease
APOE	Apolipoprotein E
ARTAG	Aging-related tau astrogliopathy
BBB	Blood-brain barrier
Braak-NFT	Braak neurofibrillary tangle
CAA	Cerebral amyloid angiopathy
cDC1	Conventional type 1 dendritic cell
CDR	Clinical Dementia Rating
CERAD	Consortium to Establish a Registry for Alzheimer's Disease
CI	Confidence interval
CNS	Central nervous system
DAB	3,3'-Diaminobenzidine tetrahydrochloride hydrate
FDR	False discovery rate
H&E	Hematoxylin and eosin
HLA	Human leukocyte antigen
HRP	Horseradish peroxidase
LATE-NC	Limbic-predominant age-related TDP-43 encephalopathy neuropathologic change
NIA-AA	National Institute on Aging-Alzheimer's Association
NFT	Neurofibrillary tangle
PART	Primary age-related tauopathy
PMI	Post-mortem interval
pTau	Hyperphosphorylated tau
RTU	Ready-to-use
SEM	Standard error of the mean
TDP-43	TAR DNA-binding protein 43

Declarations

Ethics approval and consent to participate

Autopsies were performed in accordance with the applicable laws in university or municipal hospitals in Belgium (Leuven) and Germany (Bonn and Offenbach). Recruitment protocols for collecting the human brains were approved by the ethical committees of UZ Leuven (Belgium; Decision No. S-52791, S-59292, S-59295), and the University of Ulm (Germany; Decision No. 54/08). Informed consent was obtained according to local legislation.

Consent for publication

Not applicable

Availability of data and materials

The data used, generated and analysed during the current study are available from the corresponding author on reasonable request.

Competing interests

SM has no competing interests. SO has no competing interests. RVs institution has clinical trial agreements (RV as site PI) with Alector, AviadoBio, Biogen, Bristol-Myers Squibb, Denali, EliLilly, Johnson & Johnson, Merck, Roche and UCB. RV's institution has consultancy agreements with ACImmune and Novartis (RV as Data Safety Monitoring Board or Data Monitoring Committee member), and with Roche, EliLilly and AviadoBio (RV as member of international advisory board). DRT collaborated with Novartis Pharma AG (Switzerland), Fujirebio (Belgium), and GE-Healthcare (UK) and received consultant honoraria from Muna Therapeutics (Belgium). BDS is consultant to Muna Therapeutics and is or has been consultant for Eli Lilly, Biogen, Janssen Pharmaceutica, Eisai, AbbVie and other biotech companies. B.D.S is a scientific founder of Augustine Therapeutics and a scientific founder and a minor stockholder of Muna Therapeutics.

Funding

European Research Council (ERC) under the European Union's Horizon (grant agreement no. ERC-

101199326 XenoAD ERC-2024-AdG). This work was also supported by the Flanders Institute for Biotechnology (VIB vzw), the Fonds voor Wetenschappelijk Onderzoek, the Queen Elisabeth Medical Foundation for Neurosciences, de Stichting Alzheimer Onderzoek (SAO), the Opening the Future campaign of the Leuven Universitair Fonds and the Alzheimer's Association USA, Mission Lucidity, a Medical Research Grant (MR/Y014847/1). B.D.S. holds the Bax-Vanluffelen Chair for Alzheimer's Disease. DRT received funding from Fonds Wetenschappelijk Onderzoek (FWO; Grant Nos. G065721N, G024925N) and Alzheimer's Association (USA; Grant No.: 22-AAIIA-963171).

Authors' contributions

SM: Experimental design and execution, microscopy, data analysis and interpretation, writing of the manuscript. SO: Experimental design and execution, reviewing of the paper. RV: recruitment of study participants, reviewing of the paper. DRT: interpretation, writing of the manuscript. BDS: conceptualization, interpretation, writing of the manuscript, funding.

Acknowledgements

We extend our heartfelt gratitude towards all individuals who donated their brains and their families. We thank the UZ/KU Leuven biobank (Belgium), the university hospital Bonn (Germany) and the municipal hospital Offenbach (Germany) for sharing tissue. Additional gratitude is due for Alicja Ronisz for her help in collecting the required paraffin-embedded brain samples. We also thank the bioimaging core of the Center for Neuroscience-KU Leuven (CNL) for their help with the slide scans. Finally, we thank Prof. David Holtzmann for his constructive feedback on the manuscript.

References

1. Styren SD, Civin WH, Rogers' J. Molecular, Cellular, and Pathologic Characterization of HLA-DR Immunoreactivity in Normal Elderly and Alzheimer's Disease Brain. EXPERIMENTAL NEUROLOGY. 1990.
2. De Strooper B, Sierksma A, Moechars D, Borrie S, Snellinx A, Bourdely P, et al. Polygenic risk for Alzheimer's disease shapes microglial inflammatory and antigen-presentation programs in vivo [Internet]. 2025. Available from: https://www.researchsquare.com/article/rs-7794221/v1 doi:10.21203/rs.3.rs-7794221/v1
3. De Strooper B, Borrie S, Pasciuto E, Moortel L Van, Willems P, Moechars D, et al. PICALM regulates a human microglial antigen presentation program in Alzheimer's disease [Internet]. 2026. Available from: https://www.researchsquare.com/article/rs-9701645/v1 doi:10.21203/rs.3.rs-9701645/v1
4. Lu A, Chen WT, Dalby M, Sainz Garcia D, Vanheusden M, de Vries LE, et al. Human microglial transitions at the Aβ–tau inflection point associate with divergent pathways to dementia and resilience. Nat Med. 2026 Jun 1;32(6):2047–59. doi:10.1038/s41591-026-04393-8 PubMed PMID: 42243549.
5. Thal DR, Arendt T, Waldmann G, Holzer M, Zedlick D, Rüb U, et al. Progression of neurofibrillary changes and PHF-τ in end-stage Alzheimer's disease is different from plaque and cortical microglial pathology. Neurobiol Aging. 1998 Nov;19(6):517–25. doi:10.1016/S0197-4580(98)00090-6
6. Roche PA, Cresswell P. Antigen Processing and Presentation Mechanisms in Myeloid Cells. Microbiol Spectr. 2016 May 6;4(3). doi:10.1128/microbiolspec.mchd-0008-2015 PubMed PMID: 27337472.
7. Gabitto MI, Travaglini KJ, Rachleff VM, Kaplan ES, Long B, Ariza J, et al. Integrated multimodal cell atlas of Alzheimer's disease. Nat Neurosci. 2024 Dec 1;27(12):2366–83. doi:10.1038/s41593-024-

01774-5 PubMed PMID: 39402379.

8. Mathys H, Boix CA, Akay LA, Xia Z, Davila-Velderrain J, Ng AP, et al. Single-cell multiregion dissection of Alzheimer's disease. Nature. 2024 Aug 22;632(8026):858–68. doi:10.1038/s41586-024-07606-7 PubMed PMID: 39048816.
9. Oxendine JD, Sirkis DW, Jonson C, Yokoyama JS. Single-nucleus RNA-seq reveals no increase in T cells in Alzheimer's disease prefrontal cortex or hippocampus. Front Cell Neurosci. 2025;19. doi:10.3389/fncel.2025.1681881
10. Mathys H, Peng Z, Boix CA, Victor MB, Leary N, Babu S, et al. Single-cell atlas reveals correlates of high cognitive function, dementia, and resilience to Alzheimer's disease pathology. Cell. 2023 Sep 28;186(20):4365-4385.e27. doi:10.1016/j.cell.2023.08.039 PubMed PMID: 37774677.
11. Balusu S, Horré K, Thrupp N, Craessaerts K, Snellinx A, Serneels L, et al. MEG3 activates necroptosis in human neuron xenografts modeling Alzheimer's disease. Science (1979). 2023 Sep 15;381(6663):1176–82. doi:10.1126/science.abp9556
12. Sun Z, Kwon JS, Ren Y, Chen S, Walker CK, Lu X, et al. Modeling late-onset Alzheimer's disease neuropathology via direct neuronal reprogramming. Science. 2024 Aug 2;385(6708):adl2992. doi:10.1126/science.adl2992 PubMed PMID: 39088624.
13. Klimmt J, Cardoso Gonçalves C, Montgomery JV, Müller SA, Bublitz M, Filser S, et al. A reproducible three-dimensional model of human brain tissue to investigate physiological and disease-associated microglia phenotypes. Nat Neurosci. 2026 Aug 4. doi:10.1038/s41593-026-02367-0
14. Kwak SS, Washicosky KJ, Brand E, von Maydell D, Aronson J, Kim S, et al. Amyloid-β42/40 ratio drives tau pathology in 3D human neural cell culture models of Alzheimer's disease. Nat Commun. 2020 Dec 1;11(1). doi:10.1038/s41467-020-15120-3 PubMed PMID: 32170138.
15. Choi SH, Kim YH, Hebisch M, Sliwinski C, Lee S, D'Avanzo C, et al. A three-dimensional human neural cell culture model of Alzheimer's disease. Nature. 2014 Nov 13;515(7526):274–8. doi:10.1038/nature13800 PubMed PMID: 25307057.
16. Braak H, Braak E. Neuropathological stageing of Alzheimer-related changes. Acta Neuropathol. 1991;82(4):239–59. doi:10.1007/bf00308809 PubMed PMID: 1759558.
17. Braak H, Alafuzoff I, Arzberger T, Kretzschmar H, Tredici K. Staging of Alzheimer disease-associated neurofibrillary pathology using paraffin sections and immunocytochemistry. Acta Neuropathol. 2006;112(4):389–404. doi:10.1007/s00401-006-0127-z
18. Thal DR, Rüb U, Orantes M, Braak H. Phases of Aβ-deposition in the human brain and its relevance for the development of AD. Neurology. 2002;58(12):1791–800. doi:10.1212/WNL.58.12.1791
19. Mirra SS, Heyman A, McKeel D, Sumi SM, Crain BJ, Brownlee LM, et al. The Consortium to Establish a Registry for Alzheimer's Disease (CERAD). Part II. Standardization of the neuropathologic assessment of Alzheimer's disease. Neurology. 1991 Apr;41(4):479–86. doi:10.1212/wnl.41.4.479 PubMed PMID: 2011243.
20. Hyman BT, Phelps CH, Beach TG, Bigio EH, Cairns NJ, Carrillo MC, et al. National Institute on Aging-Alzheimer's Association guidelines for the neuropathologic assessment of Alzheimer's disease.

Alzheimer's and Dementia. 2012;8(1):1–13. doi:10.1016/j.jalz.2011.10.007 PubMed PMID: 22265587.

21. Crary JF, Trojanowski JQ, Schneider JA, Abisambra JF, Abner EL, Alafuzoff I, et al. Primary age-related tauopathy (PART): a common pathology associated with human aging. Acta Neuropathol. 2014;128(6):755–66. doi:10.1007/s00401-014-1349-0 PubMed PMID: 25348064.
22. Hughes CP, Berg L, Danziger WL, Coben LA, Martin RL. A new clinical scale for the staging of dementia. British Journal of Psychiatry. 1982;140(6):566–72. doi:10.1192/bjp.140.6.566 PubMed PMID: 7104545.
23. Hecht M, Krämer LM, von Arnim CAF, Otto M, Thal DR. Capillary cerebral amyloid angiopathy in Alzheimer's disease: association with allocortical/hippocampal microinfarcts and cognitive decline. Acta Neuropathol. 2018;135(5):681–94. doi:10.1007/s00401-018-1834-y PubMed PMID: 29574591.
24. Ratner B. The correlation coefficient: Its values range between 1/1, or do they. Journal of Targeting, Measurement and Analysis for Marketing. 2009;17(2):139–42. doi:10.1057/jt.2009.5
25. McGeer PL, Itagaki S, Tago H, McGeer EG. Reactive microglia in patients with senile dementia of the Alzheimer type are positive for the histocompatibility glycoprotein HLA-DR. Neurosci Lett. 1987 Aug;79(1–2):195–200. doi:10.1016/0304-3940(87)90696-3
26. McGeer PL, Itagaki S, Boyes BE, McGeer EG. Reactive microglia are positive for HLA-DR in the substantia nigra of Parkinson's and Alzheimer's disease brains. Neurology. 1988 Aug;38(8):1285–1285. doi:10.1212/WNL.38.8.1285
27. Sasaki A, Yamaguchi H, Ogawa A, Sugihara S, Nakazato Y. Microglial activation in early stages of amyloid β protein deposition. Acta Neuropathol. 1997 Oct 12;94(4):316–22. doi:10.1007/s004010050713
28. Merlini M, Kirabali T, Kulic L, Nitsch RM, Ferretti MT. Extravascular CD3+ T Cells in Brains of Alzheimer Disease Patients Correlate with Tau but Not with Amyloid Pathology: An Immunohistochemical Study. Neurodegener Dis. 2018 Mar 1;18(1):49–56. doi:10.1159/000486200 PubMed PMID: 29402847.
29. Moreno-Valladares M, Silva TM, Garcés JP, Saenz-Antoñanzas A, Moreno-Cugnon L, Álvarez-Satta M, et al. CD8+ T cells are present at low levels in the white matter with physiological and pathological aging. Aging. 2020 Oct 13;12(19):18928–41. doi:10.18632/aging.104043
30. Unger MS, Li E, Scharnagl L, Poupardin R, Altendorfer B, Mrowetz H, et al. CD8+ T-cells infiltrate Alzheimer's disease brains and regulate neuronal- and synapse-related gene expression in APP-PS1 transgenic mice. Brain Behav Immun. 2020 Oct 1;89:67–86. doi:10.1016/j.bbi.2020.05.070 PubMed PMID: 32479993.
31. Chen X, Firulyova M, Manis M, Herz J, Smirnov I, Aladyeva E, et al. Microglia-mediated T cell infiltration drives neurodegeneration in tauopathy. Nature. 2023 Mar 23;615(7953):668–77. doi:10.1038/s41586-023-05788-0 PubMed PMID: 36890231.
32. Hu H, Lin PBC, Zeng C, Li Y, Bosch ME, Emmerson JT, et al. Priming of CD8+ T cells by peripheral dendritic cells exacerbates tau-mediated neurodegeneration. Nat Neurosci. 2026 Sep 3.

doi:10.1038/s41593-026-02427-5

33. Gate D, Saligrama N, Leventhal O, Yang AC, Unger MS, Middeldorp J, et al. Clonally expanded CD8 T cells patrol the cerebrospinal fluid in Alzheimer's disease. Nature. 2020 Jan 16;577(7790):399–404. doi:10.1038/s41586-019-1895-7 PubMed PMID: 31915375.
34. Hobson R, Levy SHS, Singal CMS, Flaherty D, Xiao H, Ciener B, et al. Clonal CD8+ T cells populate the leptomeninges and coordinate with immune cells in human degenerative brain diseases. Nat Immunol. 2026 Feb 1;27(2):323–35. doi:10.1038/s41590-025-02401-6 PubMed PMID: 41593242.
35. Hartnell IJ, Woodhouse D, Jasper W, Mason L, Marwaha P, Graffeuil M, et al. Glial reactivity and T cell infiltration in frontotemporal lobar degeneration with tau pathology. Brain. 2024 Feb 1;147(2):590–606. doi:10.1093/brain/awad309 PubMed PMID: 37703311.
36. Wekerle H, Linington C, Lassmann H, Meyermann R. Cellular immune reactivity within the CNS. Trends Neurosci. 1986;9:271–7. doi:10.1016/0166-2236(86)90077-9
37. Dhanwani R, Pham J, Premlal ALR, Frazier A, Kumar A, Pero ME, et al. T Cell Responses to Neural Autoantigens Are Similar in Alzheimer's Disease Patients and Age-Matched Healthy Controls. Front Neurosci. 2020 Aug 27;14. doi:10.3389/fnins.2020.00874

Figures

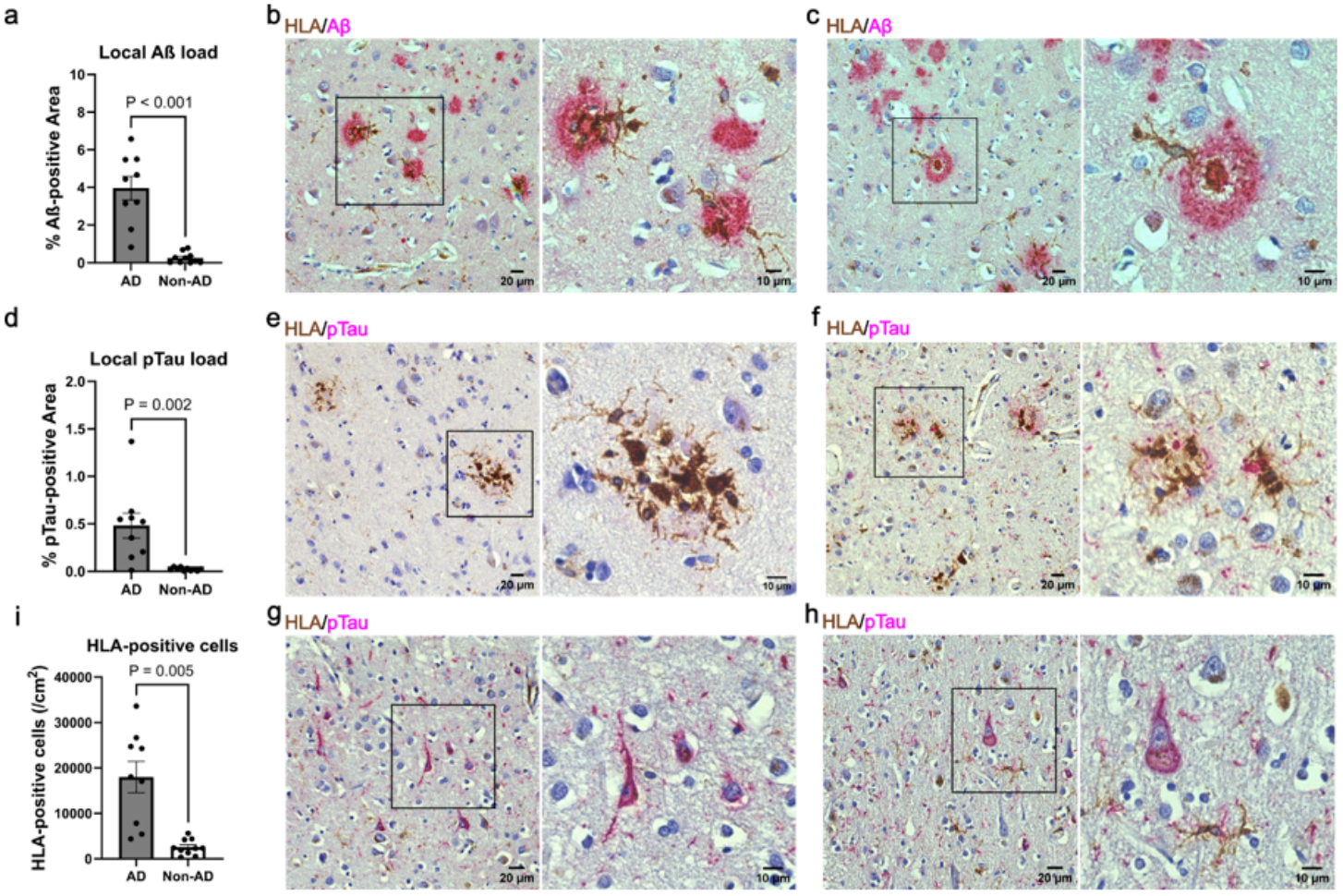


Figure 1

Expression of HLA class II in relation to local Aβ and pTau pathology in frontal cortical grey matter. Quantification of local Aβ pathology from chromogen stains, represented as percentage of positive area per case with SEM (**a**). Representative images of double chromogenic stains for Aβ (FastRed, red) together with HLA-DR/DP/DQ (DAB, brown) (**b**, **c**). Quantification of local pTau pathology from chromogen stains, represented as percentage of positive area per case with SEM (**d**). Representative images of double chromogenic stains for pTau (FastRed, red) together with HLA-DR/DP/DQ (DAB, brown) (**e**, **f**). Examples illustrate the accumulation of HLA-positive cells around Aβ plaques (**b**, **c**) and in cortical regions containing limited pTau pathology (**e**), neuritic pTau pathology (**f**), and pTau-positive neuronal cell bodies (**g** and **h**). HLA-positive cells were quantified as the number of HLA-DR/DP/DQ positive cells per cm^2 of frontal cortex grey matter (**i**). Binary logistic regression was used controlled for age and sex (n=19).

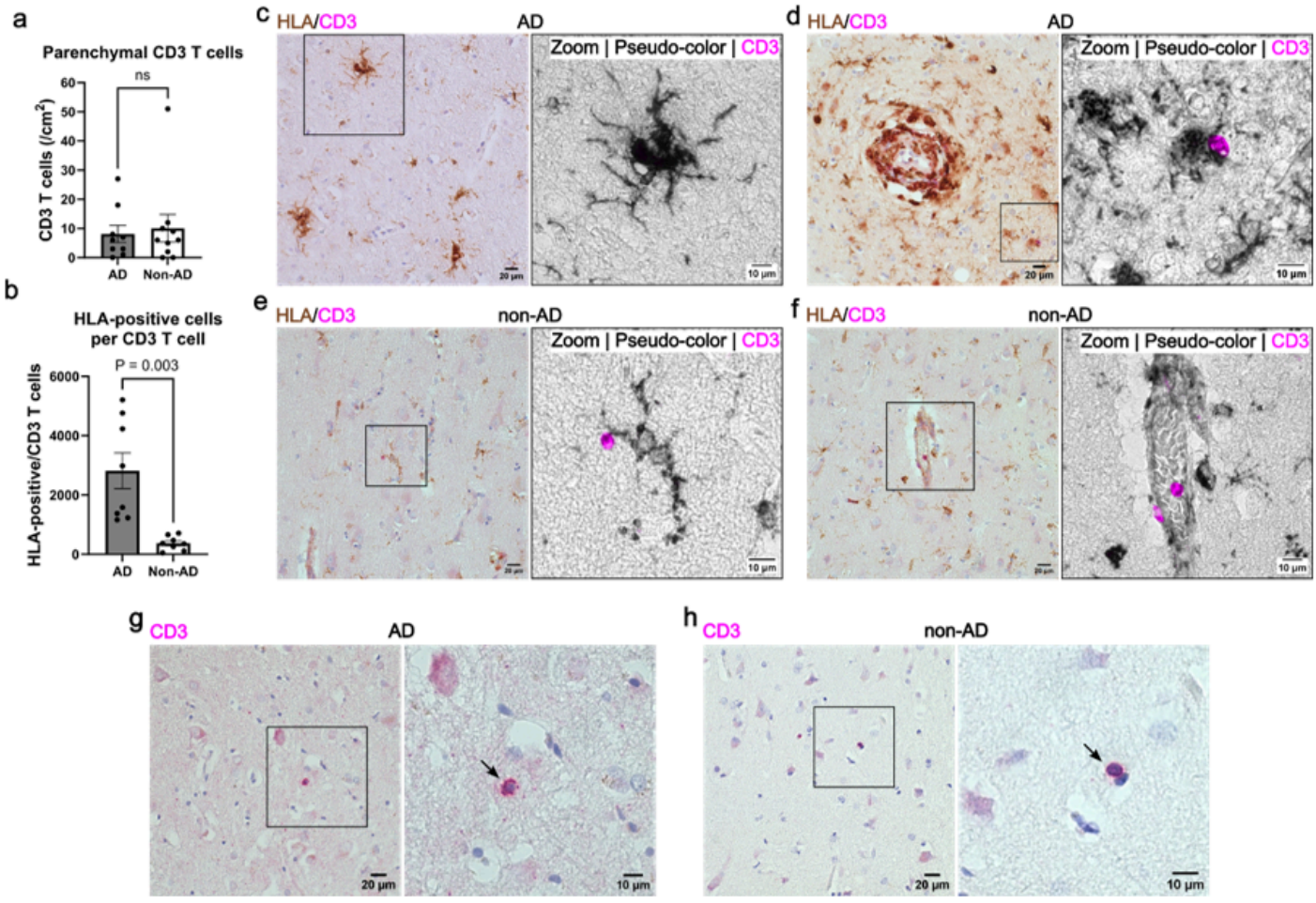


Figure 2

Increased numbers of HLA-positive cells without accumulation of CD3-positive T cells in the frontal cortex of symptomatic AD cases. Parenchymal CD3-positive T cells were quantified as the number of CD3-positive cells per cm^2 of frontal cortex grey matter (**a**). The number of cells per individual case is

shown (n=9 AD, n=10 non-AD) together with the mean and SEM. The ratio of HLA-positive cells over the number of parenchymal CD3 T cells indicates the extent of T cell abundance in context of the upregulation of HLA for cases where parenchymal CD4 T cells were observed (n=8 AD, n=8 non-AD) (**b**). Binary logistic regression was used controlled for age and sex. Representative chromogenic immunostainings for HLA-DR/DP/DQ (DAB, brown) and CD3 (FastRed, red) in symptomatic AD (**c, d**) and non-demented control cases (**e, f**). CD3 T cells are highlighted on the right-hand side of each panel using magenta pseudo-coloring, together with HLA-DR/DP/DQ shown in grey. The images illustrate the absence of CD3-positive T cells within a cluster of HLA-positive cells in an AD case (**c**), the presence of individual parenchymal CD3-positive T cells in an AD case (**d**) and non-AD case (**e**), and vascular CD3 T cells in a non-AD case (**f**). Single chromogenic stains using FastRed for CD3 (n=2 AD, n=2 non-AD) confirm the sparse presence of parenchymal CD3-positive T cells in AD and non-AD cases (**g** and **h**).

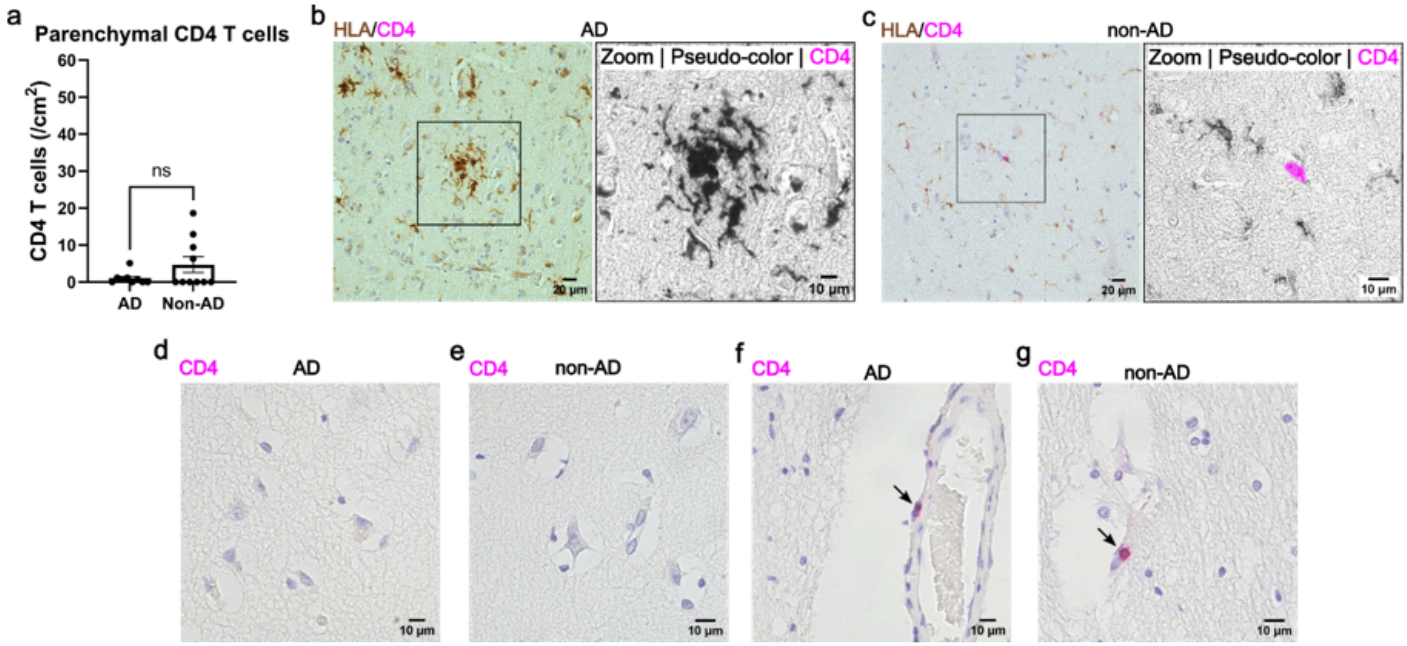


Figure 3

CD4-positive T cells are rare in symptomatic AD and non-demented control cases. Parenchymal CD4-positive T cells were quantified as the number of CD4-positive cells per cm^2 of frontal cortex grey matter (**a**). The number of positive cells per individual case is shown (n=9 AD, n=10 non-AD) together with the mean and SEM. Binary logistic regression was used controlled for age and sex. Representative chromogen immunostainings for HLA-DR/DP/DQ (DAB, brown) and CD4 (FastRed, red) in symptomatic AD (**b**), and a non-demented control case (**c**). CD4-positive T cells are highlighted on the right-hand side of each panel using magenta pseudo-coloring, together with HLA-DR/DP/DQ shown in grey. The images illustrate the absence of CD4-positive T cells within a cluster of HLA-positive cells in the AD case (**b**) and the presence of a parenchymal CD4-positive T cell in a non-AD case (**c**). Single chromogenic stains for CD4 with FastRed (n=2 AD, n=2 non-AD) confirm the scarcity of CD4-positive T cells in the parenchyma

of an AD (**d**) and non-AD (**e**) case, while vascular CD4-postive T cells are observed in association with white matter blood vessels (**f** and **g**).

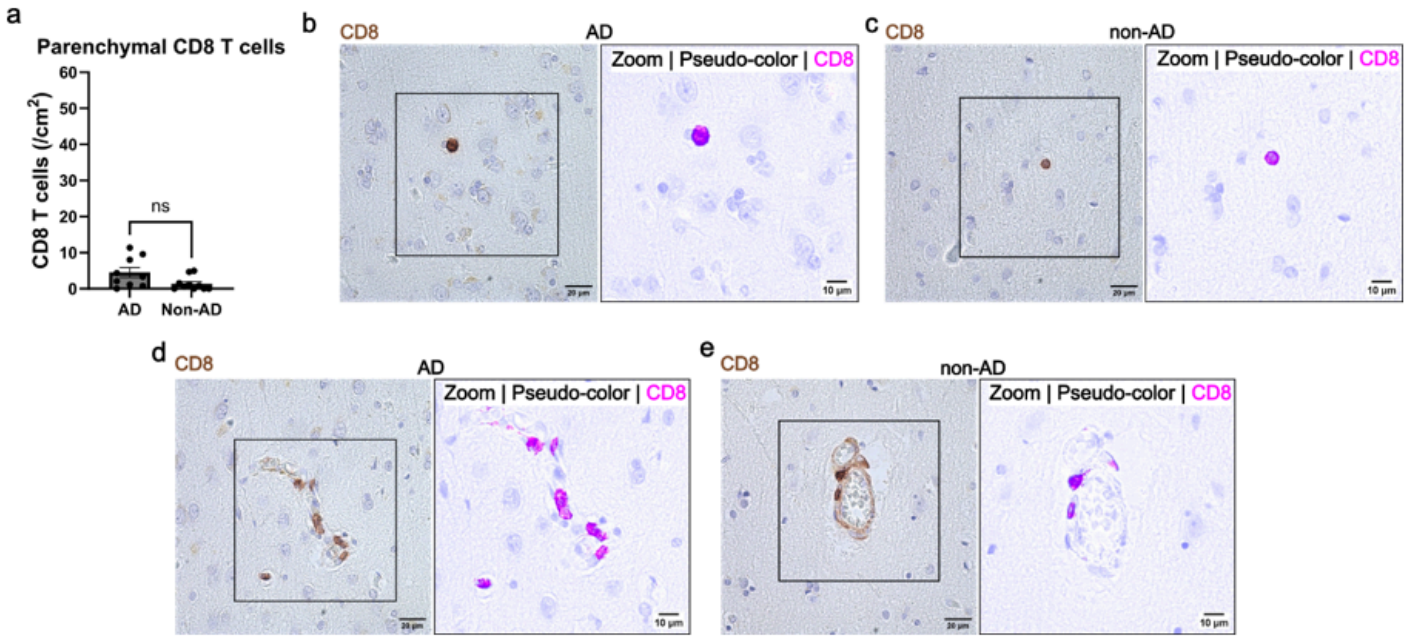


Figure 4

CD8-positive T cells in symptomatic AD and non-demented control cases. Parenchymal CD8-positive T cells were quantified as the number of CD8-positive cells per cm^2 of frontal cortical grey matter (**a**). The number of cells per individual case is shown (n=9 AD and n=10 non-AD) , together with mean and SEM. Binary logistic regression was used controlled for age and sex. Representative chromogenic immunostainings for CD8 (DAB, brown) in symptomatic AD (**b**) and a non-demented control case (**c**). CD8-positive T cells are highlighted on the right-hand side of each panel using magenta pseudo-coloring, together with the haematoxylin counterstain shown in blue. The images illustrate individual parenchymal CD8-positive T cells in an AD and non-AD case (**b** and **c** respectively) and multiple CD8-positive T cells associated with blood vessels in an AD and non-AD case (**d** and **e** respectively).

Supplementary Files

This is a list of supplementary files associated with this preprint. Click to download.

- 20261020Moonenetal2026SupplementaryTables.xlsx
- SupplementaryFigures.docx